



Enhancement of NiSi-Based Nanocrystal Formation by Incorporating Ge Elements for Nonvolatile Memory Devices

Chih-Wei Hu,^a Ting-Chang Chang,^{b,*} Chun-Hao Tu,^a Cheng-Neng Chiang,^a
Chao-Cheng Lin,^a Sheng-Wei Lee,^c Chun-Yen Chang,^a Simon M. Sze,^a
and Tseung-Yuen Tseng^a

^aInstitute of Electronics, National Chiao Tung University, Hsin-Chu 300, Taiwan

^bDepartment of Physics, Institute of Electro-Optical Engineering, and Center for Nanoscience and Nanotechnology, National Sun Yat-Sen University, Kaohsiung 804, Taiwan

^cInstitute of Materials Science and Engineering, National Central University, Tao-yuan 32001, Taiwan

In this work, a NiSiGe mixed film was deposited by the cosputtering approach. The rapidly thermal treatment condition was executed at 600°C for 30 s in nitrogen ambient to form the nanocrystal structure. From the results of the transmission electron microscopy, the annealed NiSiGe film reveals a larger nanocrystal size and density distribution than pure NiSi. X-ray photoelectron spectroscopy analyses were used to confirm that the Ge elements provide the additional nucleation centers and enhance the nanocrystal formation during the thermal process. Raman spectroscopy and an energy-dispersive spectrometer also exhibit the compositions of nanocrystals including Ni, Si, and Ge elements. With the better formation process, a remarkable improvement of memory effect is observed by comparing with the NiSi and NiSiGe nanocrystal memory devices. Also, the NiSiGe nanocrystal device shows a better retention characteristic due to the lower quantum confinement effect.

© 2009 The Electrochemical Society. [DOI: 10.1149/1.3167386] All rights reserved.

Manuscript submitted March 4, 2009; revised manuscript received June 2, 2009. Published July 22, 2009.

In recent years, the arrays of a nanocrystal (NC) structure attract much attention for several applications such as the nanoscale pattern, magnetic data storage, light emitting devices, and nonvolatile memory devices.¹⁻⁴ With the difference of the applications, finding a suitable material to satisfy the requirements is a major subject. NiSi-based NCs are considered possible materials for the current memory manufacturing technology due to their compatibility and low resistivity.^{5,6} The uniformity and density of NC distribution are also essential issues for NC formation engineering. Several methods to form a high density distribution NC structure have been proposed in previous research.^{7,8} It is disadvantageous to apply the NCs into the device process if the NC formation needs a high fabricating temperature. A self-assembly method indicates that the aggregation of NCs depends on the nucleation centers and growth rate.^{9,10} The reported literature also showed that the NC aggregation can be enhanced through diffusing additional elements to be extra nucleation centers during the NC formation.¹¹ Therefore, adjusting the compositions of the self-assembled film to increase the nucleation centers is a possible method to improve the thermal budget issue and enhance the NC formation for memory application.

In this work, the nickel-silicon-germanium (NiSiGe) mixed film was prepared by cosputtering NiSi₂ and Ge targets on a 6 in. silicon wafer with a 5 nm thermal oxide simultaneously. Rapid thermal annealing (RTA) was used to treat the stacked structure with NiSiGe and NiSi thin films. The uniformity and density of the NCs were also estimated by transmission electron microscopy (TEM). Detailed compositions of the annealed film were analyzed by X-ray photoelectron spectroscopy (XPS), Raman spectroscopy, and an energy-dispersive spectrometer (EDS) system. Then, the NC formation behaviors were speculated by the results of material analyses. We also fabricated the memory device using the NiSiGe and NiSi NCs as charge trapping layers to investigate the charge-storage ability. The excellent electrical characteristics of NiSiGe NC memory devices, such as capacitance-voltage (C-V), retention, and endurance, were also demonstrated and discussed.

Experimental

Figure 1 is the process flow of the experiment. First, a 5 nm thick oxide was grown on the p-type silicon wafer in an atmospheric pressure chemical vapor deposition (APCVD) furnace. Afterward, a

6 nm thick NiSiGe mixed film was deposited by a cosputtering approach. Then, a 20 nm thick capped oxide was deposited to form a trilayer structure by the plasma-enhanced chemical vapor deposition (PECVD) system. Subsequently, RTA at 600°C was performed for 30 s in N₂ ambient to form an NC structure. After the RTA process, a 30 nm thick blocking oxide (SiO₂) was capped by the PECVD system. Finally, an Al gate electrode was patterned to form a metal oxide-insulator-oxide silicon (MOIOS) structure. The structure with NiSi NCs was formed by the same process for comparison. After the fabrication of devices, we studied the formation of the NCs by related material analyses and the charge-storage ability of the memory devices by electrical measurements.

Results and Discussion

Figure 2a and b indicates the plane-view and cross-section TEM images of the NiSi and NiSiGe layers after the thermal annealing process, respectively. NCs were nucleated between the tunneling oxide and the blocking oxide after the annealing process. We also calculated the NC density and size from the plane-view TEM, as listed in Table I. The NiSiGe NCs reveal larger density and size distributions. The improved NiSi-based NC formation may be attributed to the help of Ge elements. To further realize the NiSiGe NC formation, the XPS spectra were used. Figure 3a demonstrates the Ni 2p_{3/2} XPS spectra of the NiSi and NiSiGe mixed films after thermal annealing. The Ni-Si signal is determined in both samples. There is less difference between the samples. The main difference in XPS spectra between annealed NiSi and NiSiGe thin films is found

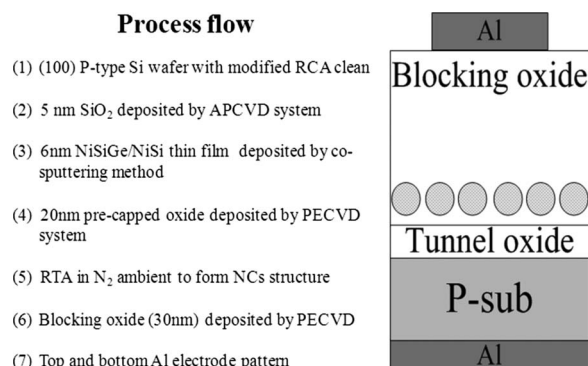


Figure 1. The process flow proposed in this work.

* Electrochemical Society Active Member.

^z E-mail: tchang@mail.phys.nsysu.edu.tw

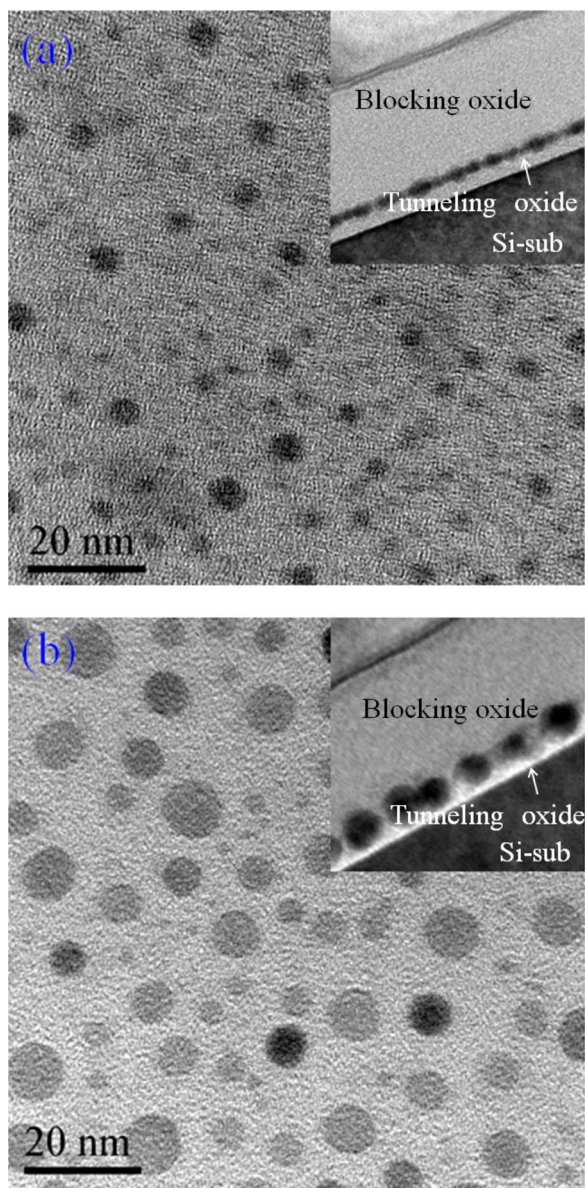


Figure 2. (Color online) The plane-view and cross-section TEM micrographs of the annealed (a) NiSi and (b) NiSiGe films.

at the Ge 3d result, as shown in Fig. 3b. The Ge–Ge peak at ~ 29.4 eV is found in Fig. 3b, which is a reference to the annealed NiSiGe sample. Furthermore, a higher binding energy is found at ~ 31.5 eV, reported by a previous literature, indicating a nickel–germane–silicide (Ni–Si–Ge) binding.¹² Hence, the NiSiGe annealing process includes Ge–Ge, Ni–Si, and Ni–Si–Ge formations. A peak at 29.4 eV appears because partial Ge elements tend to segregate out at a high temperature thermal process.¹³ It is believed that the unobvious Ni 2p_{3/2} XPS binding energy shift in the annealed

NiSiGe film is because of the small difference in binding energy between Ni–Si and Ni–Si–Ge. Then, it is difficult to recognize the difference between the samples.

Figure 4a shows the Raman spectra of the annealed NiSiGe samples. For the annealed NiSiGe film, there is a broad peak at about 220 cm^{-1} , corresponding to the Ni–Si–Ge phase. A Ge–Ge peak at about 300 cm^{-1} was found at 600°C thermal annealed samples.¹⁴ The EDS analysis was used to analyze the compositions of the NCs, as shown in Fig. 4b. The electron beam of the EDS analysis was focused at the NC region at about 10 nm. The NCs are composed of Ni, Si, and Ge elements. Through the results of the material analyses, the main composition of the NCs is not pure NiSi₂ because the Ge can be the initial nucleation centers to form the NCs. Compared with the NiSi mixed film, the NiSiGe layer offers more additional nucleation centers for the NC formation. Therefore, the NiSiGe film provides a more complete nucleation process and induces a larger size and density distribution at a lower fabricating temperature.

The detailed nucleation of NiSi-based NCs during the RTA process is speculated, as shown in Fig. 5. From the reported literature, the Ge elements tend to precipitate during the thermal annealing.¹⁵ In the NiSi film, NiSi₂ and Ge serve as nucleation centers at the initial thermal annealing process. For the detailed compositions, the starting clusters include Ge–Ge and Ge–O, which are evidenced from the XPS analysis, as shown in Fig. 3b. The additional nucleation centers enhance the NC nucleation and bring a larger density in the annealed NiSiGe sample. The advantage of the addition of the Ge elements also involves a low temperature process. The characteristics, such as density and size, of the NiSiGe NC formation at 600°C are superior to the conventional NiSi NC formation at 700°C . Hence, the NiSi-based NCs with a better size and density distribution can be obtained at a lower temperature by adding Ge elements.

To study the feasibility of the NiSiGe NCs to apply into the memory devices, the MOIOS structure had been fabricated and measured. Figure 6 shows the *C-V* hysteresis after bidirectional sweeps, which implies the electron charging and discharging effect of the memory device. In Fig. 6a, the conventional NiSi NC memory device shows a flatband voltage (V_{FB}) shift of 4.5 V under a ± 10 V gate voltage operation. In contrast to the NiSi NCs, the NiSiGe NC memory device exhibits a 9 V flatband voltage shift in Fig. 4b. The larger memory device of NiSiGe, defined as “1” or “0” for the logic-circuit design, results from the improved NC size and density distribution. An early nuclei formation can bring a larger NC size and better uniformity distribution to improve the charge-storage performance of the memory device.

Figure 7 shows the data retention characteristic of (a) NiSi NC and (b) NiSiGe NC devices. The NiSiGe NC device reveals better data retention ability than the NiSi NCs after 10^4 s. The retention characteristic is better because the NiSiGe NCs have a lower quantum confinement effect due to the larger NC size distribution. According to the reported literature, the NCs (< 2 nm) are difficult to apply into the NC memory devices because the quantum confinement effect depends on the NC size strongly.^{16,17} The better uniformity of NiSiGe NCs can reduce the possibility that the stored charge tunnels back during the retention test. Also, charge-storage decay is obvious at the initial 10^3 s for the NC devices. The decay is probably because the charges stored in the shallow traps are easy to lose. Nevertheless, both the NiSi and NiSiGe NC memory devices can keep steady after the decay. Figure 8 shows the endurance characteristics of the NiSi and NiSiGe NC memory. After 10^6 operation cycles, the performance of the NC memory devices reveals an unobvious degradation. The endurance behavior is probably related to the quality of the tunneling oxide, which was deposited by the same APCVD process in our experiment. Therefore, the devices show similar characteristics for the endurance test. Moreover, it is confirmed that the additional Ge does not degrade the quality of the

Table I. A list of the formed NC density and size calculated by the TEM images.

	Annealing temperature ($^\circ\text{C}$)	NC size (nm)	NC density (cm^{-2})
NiSi	700	2–3	3.02×10^{11}
NiSiGe	600	8–9	4.95×10^{11}
	700	12–13	2.54×10^{11}

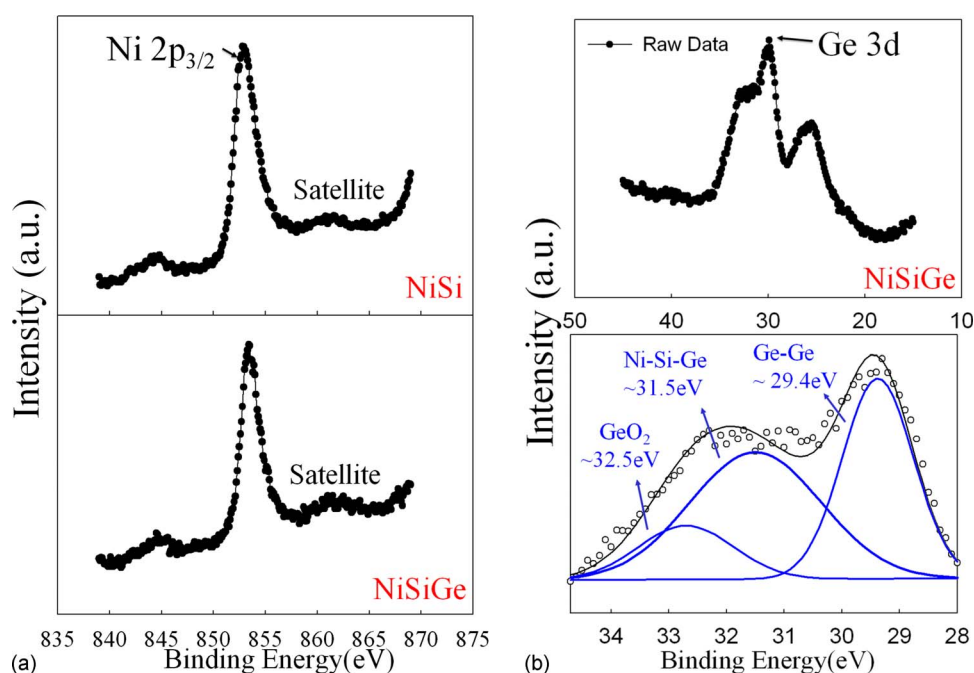


Figure 3. (Color online) (a) The Ni 2p_{3/2} XPS spectra of the annealed NiSi and NiSiGe mixed film. (b) The Ge 3d XPS spectra raw data and the fitting data of the NiSiGe film after thermal annealing.

tunneling oxide and obviously affects the reliability of the NC memory devices.¹⁸ An adequate reliability characteristic can be provided by the NiSiGe NCs for the application of nonvolatile memory devices.

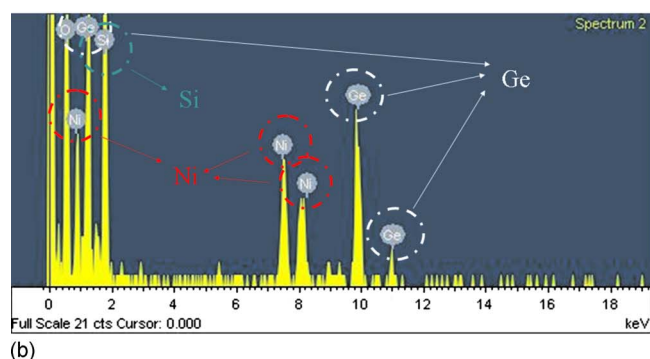
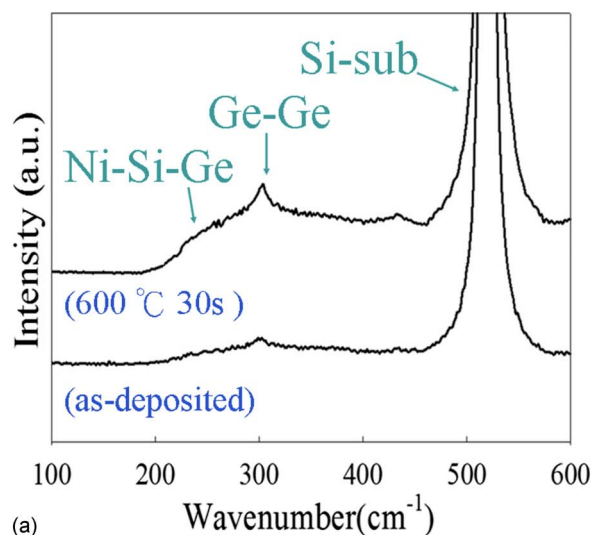


Figure 4. (Color online) (a) Raman spectroscopy and (b) EDS of the NiSiGe film after thermal annealing.

Conclusion

The formation of NCs has been studied by incorporating Ge elements into NiSi. Better uniformity and density are found in the annealed NiSiGe samples. It results from the fact that the Ge elements offer more nucleation centers to help the formation of the NCs. The incorporated Ge method with a lower thermal budget applies to the current device fabrication. We also demonstrate the NiSiGe NCs memory devices formed by annealing the NiSiGe film. The NiSiGe NCs memory device shows a superior memory window to the conventional NiSi NCs due to the improved formation process. The better size and uniformity of NCs is the principal reason for the improved charge-storage ability. We also tested the reliability characteristic of the NiSiGe NC memory device by retention and

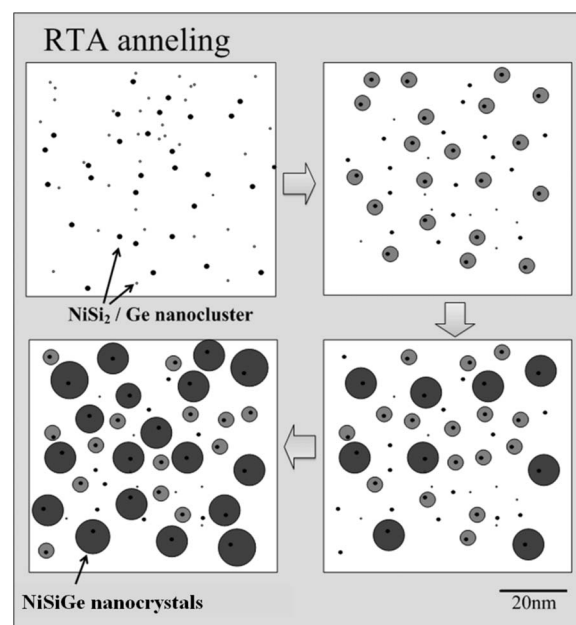


Figure 5. The speculated picture for the formation process of the NiSiGe NCs during RTA process.

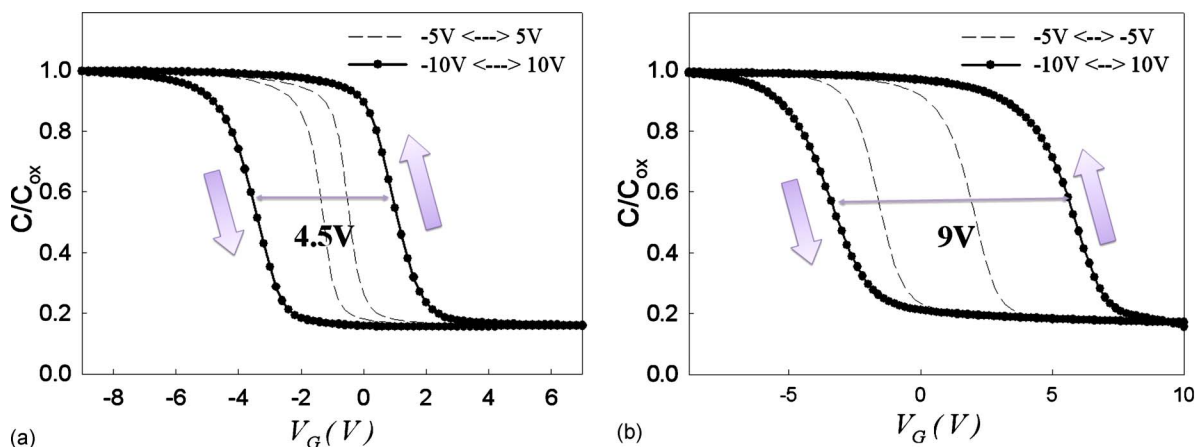


Figure 6. (Color online) C-V characteristics (1 MHz) of the MOIOS structures with (a) NiSi and (b) NiSiGe NCs as the trapping layers of the memory device.

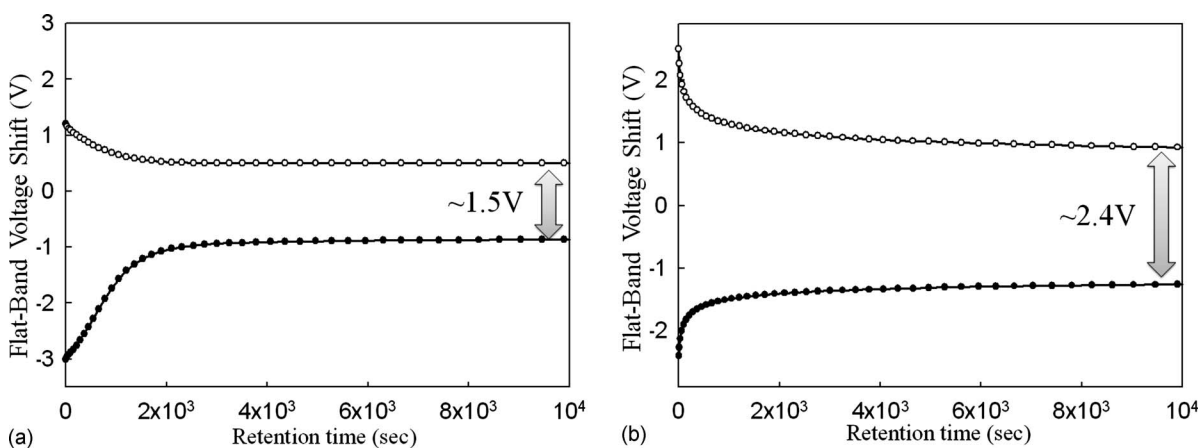


Figure 7. Retention characteristics of the (a) NiSi and (b) NiSiGe NC memory devices.

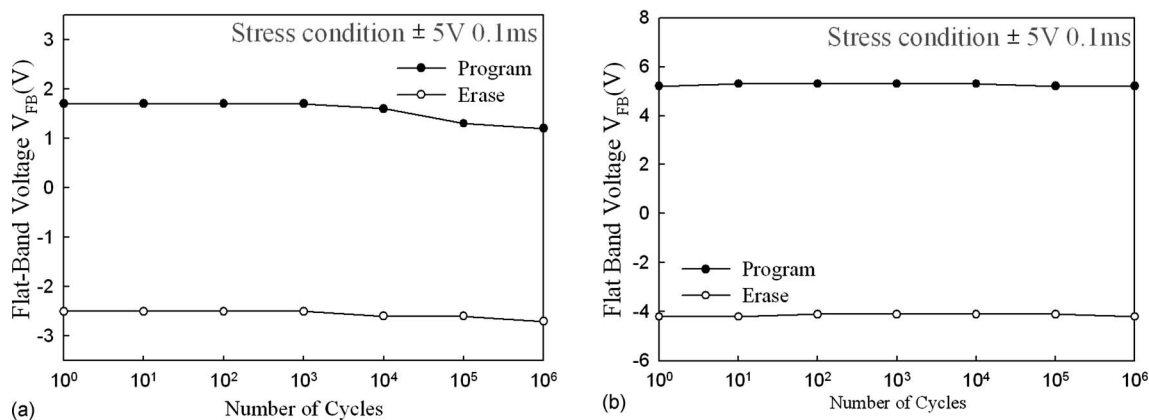


Figure 8. Endurance characteristics of the (a) NiSi and (b) NiSiGe NC memory devices.

endurance measurements. The good reliability characteristic of the NiSiGe NC device is also advantageous to the memory devices.

Acknowledgment

This work was performed at the National Nano Device Laboratory and was supported by the National Science Council of Taiwan under contract no. NSC 97-2112-M-110-009, no. NSC 97-2221-E-009-151, no. NSC 97-2221-E-009-148, and no. NSC 97-3114-M-110-001.

National Sun Yat-Sen University assisted in meeting the publication costs of this article.

References

1. G. R. Lin, C. J. Lin, H. C. Kuo, H. S. Lin, and C. C. Kao, *Appl. Phys. Lett.*, **90**, 143102 (2007).
2. H. Wang, Y. Chen, H. B. Wang, C. Zhang, F. J. Yang, J. X. Duan, C. P. Yang, Y. M. Xu, M. J. Zhou, and Q. Li, *Appl. Phys. Lett.*, **90**, 052505 (2007).
3. J. M. Moon, J. H. Bae, J. A. Jeong, S. W. Jeong, N. J. Park, H. K. Kim, J. W. Kang, J. J. Kim, and M. S. Yi, *Appl. Phys. Lett.*, **90**, 163516 (2007).
4. S. Tiwari, F. Rana, K. Chan, H. Hanafi, W. Chan, and D. Buchanan, *Tech. Dig.* -

- Int. Electron Devices Meet.*, **1995**, 521.
5. Z. Liu, C. Lee, V. Narayanan, G. Pei, and E. C. Kan, *IEEE Trans. Electron Devices*, **49**, 1606 (2002).
 6. Z. Tan, S. K. Samanta, W. J. Yoo, and S. Lee, *Appl. Phys. Lett.*, **86**, 013107 (2005).
 7. Y. Nakamura, Y. Nagadomi, K. Sugie, and N. Miyata, *J. Appl. Phys.*, **95**, 5014 (2004).
 8. J. H. Chen, W. J. Yoo, D. S. H. Chan, and L. J. Tang, *Appl. Phys. Lett.*, **86**, 073114 (2005).
 9. D. Aurongzeb, S. Patibandla, M. Holtz, and H. Temkin, *Appl. Phys. Lett.*, **86**, 103107 (2005).
 10. H. G. Chew, W. K. Choi, Y. L. Foo, F. Zheng, W. K. Chim, Z. J. Voon, K. C. Seow, E. A. Fitzgerald, and D. M. Y. Lai, *Nanotechnology*, **17**, 1964 (2006).
 11. L. Bi, Y. He, J. Y. Feng, and Z. J. Zhang, *Nanotechnology*, **17**, 2289 (2006).
 12. S. K. Ray, T. N. Adam, G. S. Kar, C. P. Swann, and J. Kolodzey, *Mater. Res. Soc. Symp. Proc.*, **745**, N6.6.1 (2003).
 13. H. B. Yao, M. Bouville, D. Z. Chi, H. P. Sun, X. Q. Pan, D. J. Srolovitz, and D. Mangelinckd, *Electrochem. Solid-State Lett.*, **10**, H53 (2007).
 14. K. L. Pey, W. K. Choi, S. Chattopadhyay, H. B. Zhao, E. A. Fitzgerald, D. A. Antoniadis, and P. S. Lee, *J. Vac. Sci. Technol. A*, **20**, 1903 (2002).
 15. W. K. Choi, V. Ng, S. P. Ng, H. H. Thio, Z. X. Shen, and W. S. Li, *J. Appl. Phys.*, **86**, 1398 (1999).
 16. Y. Nakayama, I. Matsuda, S. Hasegawa, and M. Ichigawa, *Appl. Phys. Lett.*, **88**, 253102 (2006).
 17. M. She and T. J. King, *IEEE Trans. Electron Devices*, **50**, 1934 (2003).
 18. T. H. Ng, W. K. Chim, W. K. Choi, V. Ho, L. W. Teo, A. Y. Du, and C. H. Tung, *Appl. Phys. Lett.*, **84**, 4385 (2004).